Experimental and Molecular Pathology 107 (2019) 32–42

Contents lists available at ScienceDirect

Experimental and Molecular Pathology

journal homepage: www.elsevier.com/locate/yexmp

Aluminum disrupts the prenatal development of the male and female gerbil prostate (*Meriones unguiculatus*)

Liana S. Gomes[a], Janaína R. Costa[a], Mônica S. Campos[a], Mara R. Marques[a], Manoel F. Biancardi[a], Sebastião R. Taboga[b], Paulo C. Ghedini[c], Fernanda C.A. Santos[a,*]

[a] Department of Histology, Embryology and Cell Biology, Laboratory of Microscopy Applied to Reproduction, Institute of Biological Sciences, Federal University of Goiás, Goiânia, Goiás 74001970, Brazil
[b] Department of Biology, Laboratory of Microscopy and Microanalysis, University Estadual Paulista – UNESP, Rua Cristóvão Colombo, 2265, São José do Rio Preto, São Paulo 15054000, Brazil
[c] Department of Pharmacology, Laboratory of Molecular and Biochemistry Pharmacology, Institute of Biological Sciences, Federal University of Goiás, Goiânia, Goiás 74001970, Brazil

ARTICLE INFO

Keywords:
Metalloestrogen
Antiandrogens
Androgen receptor
Estrogen receptor alpha
Ventral prostate
Female prostate

ABSTRACT

Normal prostate development is highly dependent of an equilibrated hormonal regulation, so that sensible interferences during this period may predispose the gland to lesions during aging. Industrial activities have increased the exposure of this gland to active elements found in environment, such as aluminum (Al). Al presents toxic effect for living beings, having the potential to disrupt the development and growth of several organs and systems. Therefore, the aim of this study was to evaluate whether the prenatal exposure to Al may alter the development and morphophysiology of the gerbil prostate (*Meriones unguiculatus*). Pregnant females were orally exposed to aluminum chloride (100 mg/kg/day) from 17th to 21th gestational day. Following the birth, the male and female pups were euthanized with 1 (PN1) and 90-days-old (PN90). The prostates were collected for biometrical, three-dimensional reconstruction, morphometrical, stereological, and immunohistochemical analysis. Results indicated that Al decreases the body weight of PN1 males and females, and also reduce the anogenital distance of PN1 females. Moreover, Al changed the prostate developmental patterns of PN1 animals, causing an increase in proliferative status and decreasing androgen receptor immunostaining. The results suggest that Al-promoted changes were permanent, since low androgen receptor frequency, increased serum testosterone levels and high proliferation index were observed in adult gerbils. This study demonstrated that body and prostatic changes were more pronounced in females than in males, and that Al performed as an endocrine-disrupting chemical in gerbils.

1. Introduction

Aluminum (Al) is the most profuse metallic element found in earth crust, being present as several chemical forms in soil, water and air (Nampoothiri et al., 2017). Al salts are present in industry, civil construction, kitchen dishes, water, food, personnel products and medicine (Oda, 2016). Examples of different Al forms include aluminum oxide, aluminum chlorohydrate, aluminum hydroxide, aluminum chloride and aluminum phosphate (Cardiano et al., 2017).

The main absorption ways of the Al include inhalation, ingestion and dermal contact (Mouro et al., 2018). Through oral diet, an adult ingest almost 5–40 mg of Al daily (Yokel and McNamara, 2001). However, according to the Joint FAO/WHO Expert Committee on Food Additives (JECFA), the accepted limit for Al ingestion corresponds with 2 mg/kg/week (Crisponi et al., 2013).

Although the gastrointestinal absorption of Al is relatively low, the

Abbreviations: AGD, anogenital distance; Al, aluminum; $AlCl_3$, aluminum chloride; AR, androgen receptor; DAB, diaminobenzidine; EB, epitelial buds; ERα, estrogen receptor alpha; G0, gestational day zero; G17, 17th day of gestation; G24, 24th day of gestation; HE, hematoxylin-eosin method; JECFA, Joint FAO/WHO Expert Committee on Food Additives; MGMT, O^6-methylguanine-DNA methyltransferase; PaM, paraurethral mesenchyme; PBS, phosphate buffer saline; PCNA, proliferating cell nuclear antigen; PeM, periurethral mesenchyme; PN1, one day of post-natal life; PN90, ninety days of post-natal life; PrC, prostate complex; SM, smooth muscle; UGS, urogenital sinus; VMP, ventral mesenchymal pad; VP, ventral prostate

* Corresponding author at: Department of Histology, Embryology and Cell Biology, Laboratory of Histophysiology, Federal University of Goiás, Campus II Samambaia, Goiânia, Goiás 74001970, Brazil.
E-mail address: fernanda_alcantara@ufg.br (F.C.A. Santos).

https://doi.org/10.1016/j.yexmp.2019.01.005
Received 28 November 2018; Received in revised form 13 December 2018; Accepted 15 January 2019
Available online 17 January 2019
0014-4800/

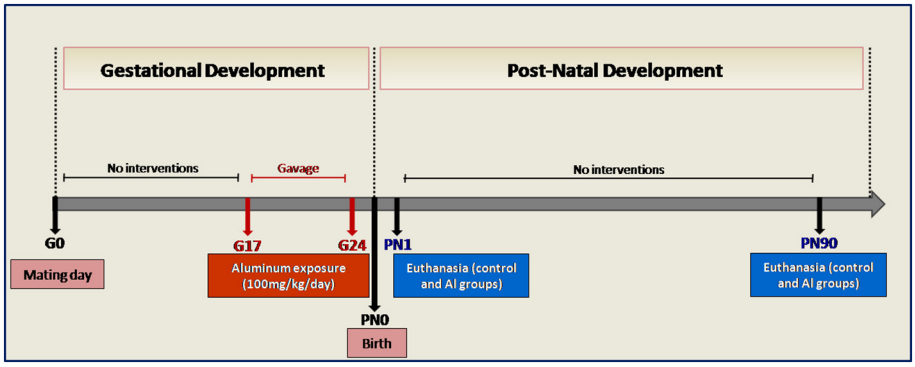

Fig. 1. Schematic representation of the experimental protocol employed in this study. The interval between G0 (day of mating) and PN0 (day of birth) represents the gerbil gestational period. The interval between G17 and G24 represent the days of aluminum exposure. The PN1 and PN90 represents the euthanasia period.

exposure to biologically active forms has been increased, mainly in pregnant, newborns, and children (Callan et al., 2013; Fanni et al., 2014). When absorbed, the Al ions accumulate inside brain, bones, liver, and kidneys, disturbing processes of cell signaling and growth (Dhivya Bharathi et al., 2018).

Recent researches with animals and human models have demonstrated the toxicant potential of Al, and its participation in the development of several pathologies, such as bone disturbances, anemia, and neurodegenerative diseases including Alzheimer, Parkinson, and encephalopathies (Lifeng et al., 2013; Erazi et al., 2016; Zhu et al., 2016; Nampoothiri et al., 2017; Zahedi-Amiri et al., 2018).

Several studies have been shown the hazardous potential of Al in development and physiology of reproductive system (Domingo, 1995; Mouro et al., 2018). Researches with mice and rats confirmed the embryotoxic and teratogenic effects of Al (Benett et al., 1975). Adult females exposed to Al presented injured ovary, which caused a disrupting of several enzymes and hormones involved either in oxidative metabolism or normal ovary function (Fu et al., 2014). In male rodents, the exposure to Al promoted testis lesions in association with hormonal imbalances (Sun et al., 2011; Zhu et al., 2014; Falana et al., 2017). However, there is a lack of studies evaluating the effects of Al exposure on the prostate.

The prostate is an accessory gland of mammal reproductive system. The development, growing, and prostate secretory function are regulated mainly by steroids hormones (Marker et al., 2003). This gland is also found in female rodents and women, and is called female prostate or Skene's paraurethral gland (Zaviacic and Ablin, 2000; Flamini et al., 2002; Santos et al., 2006; Perez et al., 2016).

Studies have demonstrated that the exposure to environmental compounds during critical phases of development leads to permanent changes in prostate morphophysiology (Hond and Schoeters, 2006; Prins et al., 2008; Lima et al., 2015). Moreover, researches showed that several metals may exert estrogenic activities when in contact with organism. These substances are referred as metalloestrogens (Darbre, 2006). Since is known that pregnant women ingest high quantity of Al due the use of antacids for dyspepsia treatment (Domingo, 1995; Fanni et al., 2014), it is important to evaluate if the consumption of Al during gestational period may cause toxicity on the prostate development of the fetuses. Therefore, the aim of this study was to evaluate the effects of gestational exposure to Al on prostate development in newborn and adult male and female gerbils *(Meriones unguiculatus)*.

2. Material and methods

2.1. Animals and experimental design

The animals were provided by the São Paulo State University (UNESP; São José do Rio Preto) and maintained under controlled conditions of light and temperature. To avoid exposing the animals to endocrine-disrupting chemicals, all animals were housed in new polyethylene cages and filtered water was provided from glass bottles. Gerbils were fed with rodent food *ad libitum* (Presence, Labina-Purina®; composition: 23% proteins, 4% fats, 5% fibers and 12% minerals). Animal handling and experiments were approved by the Institutional Ethics Committee of the Federal University of Goiás (CEUA-UFG 110/15).

We used 20 adult female and 20 adult male gerbils (*Meriones unguiculatus*, Muridae: Gerbillinae), all between 3 and 4 months old, for mating. We randomly matched one male to one female to form independent families. The mating day was determined by the presence of spermatozoa in the vaginal smears; this day was considered as gestational day zero (G0), being the initial day of the gestational period (Sanches et al., 2014). Two experimental groups were formed, as follows: Control group: ten pregnant females received oral doses of 0.9% saline solution from the 17th (G17) until the 24th day of gestation (G24); Aluminum group (Al): Ten pregnant females received oral doses of aluminum chloride ($AlCl_3$, Sigma catalogue n° 06220/Fluka, purity ≥99.0%, LD_{50}: 3450 mg/kg) from the G17 until G24 (100 mg/kg/day diluted in 0.9% saline solution – 20.2 mg Al/kg/day; 1/35 LD_{50}).

Aluminum dose employed in this work was based on the study performed by Sun et al. (2011). After the birth, males and females were separated and the gerbils were euthanized at either one (PN1) or ninety days of post-natal life (PN90) (Fig. 1). All pups (n = 8/group) were weighed and immediately euthanized by decapitation. Pups anogenital distance (AGD) was measured, and then the prostate was dissected out. Adult animals (90 days old; n = 8/group) were euthanized by cervical dislocation. The body weight and prostatic complex (PrC – correspondent urethral segment, ventral, dorsolateral, and dorsal prostate lobes in males; urethral segment, corresponding vaginal segment and prostatic ducts and alveoli for females) were weighed. These fragments were dissected out using a Leica stereoscopic microscope (Leica, Germany).

2.2. Light microscopy

The prostate glands were fixed by immersion in methacarn (methanol, chloroform and acetic acid - 6:3:1) for three hours at 4 °C, or 4% paraformaldehyde (buffered in 0.1 M phosphate, pH 7.2) for 24 h. After fixation, the tissues were washed in water, dehydrated in ethanol series, clarified in xylene, embedded in paraffin (Histosec, Merck, Darmstadt, Germany), and sectioned at 5 µm on a Leica microtome (Leica RM2155, Nussloch, Germany). The sections were stained by hematoxylin-eosin (HE). The histological sections were glued on glass slides with Entellan mounting medium (Merck, Darmstadt, Germany). The specimens were analyzed using Zeiss Axioscope A1 light microscope (Zeiss, Germany), and the images were digitalized using CellSens Standard software v1.6 (Olympus, Japan).

Table 1
Biometrical and stereological data obtained for the male and female prostate during $AlCl_3$ treatment.

	Male		Female	
	Control	Al	Control	Al
[a]Biometry				
One-day-old				
Body weight (g)	3.8 ± 0.14	3.3 ± 0.09*	3.4 ± 0.08	2.9 ± 0.07*
AGD (mm)	0.83 ± 0.03	0.81 ± 0.05	0.47 ± 0.03	0.25 ± 0.01*
Ninety-days-old				
Body weight (g)	62.5 ± 2.8	67.0 ± 1.0	51.8 ± 1.6	62.3 ± 3.4*
PrCweight (g)	0.73 ± 0.08	0.87 ± 0.04	0.16 ± 0.02	0.22 ± 0.01
PrC relative weight ($x10^{-3}$)	11.5 ± 1.0	13.0 ± 0.5	3.1 ± 0.3	3.5 ± 0.1
[b]Stereology (%)				
One-day-old				
Epithelial buds	25.4 ± 1.6	31.0 ± 1.3*	15.2 ± 0.7	19.2 ± 1.0*
Mesenchyme	56.1 ± 1.5	44.7 ± 1.7*	65.3 ± 1.2	60.4 ± 1.4*
Smooth muscle	18.5 ± 1.2	24.3 ± 1.7*	19.5 ± 1.3	20.4 ± 1.2
Ninety-days-old				
Epithelium	19.5 ± 3.0	24.8 ± 1.6*	19.4 ± 1.3	27.5 ± 1.5*
Lumen	58.0 ± 2.6	49.7 ± 3.2	36.4 ± 3.5	28.3 ± 3.9
Stroma	14.2 ± 1.1	13.3 ± 1.6	27.8 ± 1.6	29.2 ± 2.3
Smooth muscle	8.3 ± 0.7	12.2 ± 1.1*	16.4 ± 1.9	15.0 ± 1.3

[a] Anogenital distance (AGD) and body, prostate complex (PrC), and relative PrC weight in control and Al-treated gerbils ($n = 8$/group). Relative weight corresponds to the ratio between PrC and body weight. Values are means ± standard error of the means (SEM).

[b] Stereological data obtained for the male and female prostate during Al treatment (mean ± SEM; $n = 30$ fields in 5 animals/group).

* Statistically significant differences between control and Al group ($p \leq .05$).

2.3. Three-dimensional reconstruction

Three-dimensional reconstruction was performed to determine the pattern of prostatic budding and branching in both male and female PN1 gerbils ($n = 1$ animal/group). Serial histological sections were obtained from the urogenital sinus (UGS) and further stained by HE. The serial sections were sequentially digitalized. The alignment and the reconstruction of the UGS structures were performed with the Reconstruct software (Fiala, 2005). Digital images were submitted to morphometric analysis of the developing prostate buds. We determined the number, area, and sectional perimeter of epithelial outgrowths buds (ventral in males and paraurethral in females). These parameters of the male and female prostate epithelial buds were determined as the sum of all buds in a central section of each gland ($n = 5$ prostates/group).

2.4. Stereology

The stereological analyses were carried out using Weibel's multipurpose graticulate with 130 points and 10 test lines (Weibel, 1963) to compare the relative frequency of each component of prostatic tissue, as described by Vilamaior et al. (2006). We chose 30 microscopic fields at random from each experimental group (six fields per animal; $n = 5$). We determined the relative values by counting the coincident points in the test grid and dividing them by the total number of points. Stereological analysis was performed using Image-Pro Plus software v6.1 for Windows (Media Cybernetics Inc., Silver Spring, MD, USA).

2.5. Immunohistochemistry

Tissue sections were subjected to immunohistochemistry to detect androgen receptor (AR), estrogen receptor-alpha (ERα), proliferating cell nuclear antigen (PCNA), and O^6-methylguanine-DNA methyltransferase (MGMT) ($n = 3$ animals/group). The sections were deparaffinized, rehydrated through alcohol of decreasing series, and antigen retrieval was performed in a citrate buffer (pH 6.0). For detection of primary antibodies, the Leica BIOSYSTEMS NovoLink Polymer Detection System (RE7150-K, United Kingdom) kit was used. This comprises sequential stages interspersed with washing steps, which were made with phosphate buffer saline (PBS). Endogenous peroxidase activity was neutralized with Novocastra Peroxidase Block (3% hydrogen peroxide with stabilizers), and after Novocastra Protein Block (0.4% casein in PBS with stabilizers) was used to reduce the non-specific binding of the primary antibody and polymer. Primary antibodies reactive to AR (rabbit polyclonal IgG, N-20, sc-816, Santa Cruz Biotechnology, Santa Cruz, CA, USA), ERα (rabbit polyclonal IgG, MC-20, sc-542, Santa Cruz Biotechnology), PCNA (mouse monoclonal IgG_{2a}, SC 56, Santa Cruz Biotechnology, CA, USA) and MGMT (mouse monoclonal, clone E-1, SC-166528, Santa Cruz Biotechnology, CA, USA) were employed at a dilution of 1:100 overnight at 4 °C. On the next day, Novocastra Post Primary (rabbit anti mouse IgG) and Novolink™ Polymer (anti-rabbit Poly-HRP-IgG) were used as secondary antibodies. The sections were stained with DAB Chromogen (1.74% *w/v* 3,3′-diaminobenzidinem in a stabilizer solution) and Novolink™ DAB Substrate Buffer (Polymer: buffered solution containing ≤0.01% hydrogen peroxide and preservative) (proportion 1:20), and finally counterstained with Hematoxylin. The histological sections were analyzed using a Zeiss Axioscope A1 light microscope (Zeiss, Germany).

2.6. AR, ERα and PCNA quantification

For AR, ERα, and PCNA quantification, 20 microscopic fields ($n = 3$ animals/group; magnification of 400×) were used for each experimental group. In each field, the total number of positive epithelial, stromal, and mesenchymal cells was obtained as a relative frequency (%) in relation to the total number of cells. In the AR quantification, between positive and negative cells, we counted 46,573 cells; for ERα quantification we counted 14,911 cells; and, in PCNA quantification, we counted 28,357 cells. All these analyses were performed using the image analysis system previously described.

2.7. Serum testosterone dosage

Blood samples of male and female PN90 gerbils were obtained by cardiac puncture immediately after euthanasia ($n = 6$ animals/group). We were unable to obtain sufficient blood volume for the dosages of PN1 gerbils. Serum was obtained by centrifugation (1200 *g*, 20 min) and stored at −20 °C. Circulating serum testosterone levels were obtained by Competitive Enzyme immunoassay (Monobind Inc., AccuBind, Lake Forest, USA). Testosterone sensitivity was 0.0576 ng/ml.

2.8. Statistical analyses

The hypothesis tests employed to determine statistical significance were the Mann–Whitney *U* test for non-parametric distributions and the *t*-test for parametric distributions. The data were analyzed using Statistica 7.0 software (StarSoft, Inc., Tulsa, OK, USA). The level of significance was set at 5% ($p \leq .05$). Values are presented as mean ± standard error of mean (SEM).

3. Results

3.1. Biometry

Intrauterine exposure to Al significantly decreased the body weight of newborn male and female. We also observed a reduction of the AGD in females of PND1 group. Between adult animals, only the females of

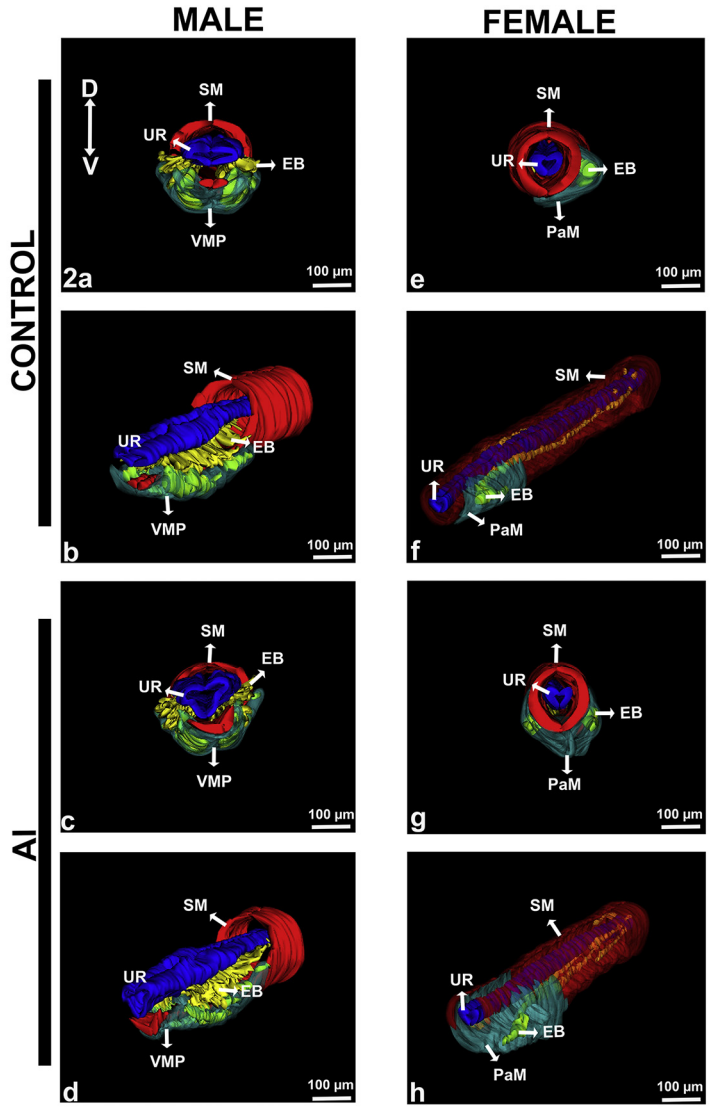

Fig. 2. Three-dimensional reconstruction model of one-day-old gerbil prostate. Ventral prostate in control (a, b) and Al-treated male gerbil (c, d). Paraurethral glands in control (e, f) and Al-treated female gerbil (g, h). Blue: urethral epithelium (UR); yellow: epithelial buds (EB); red: smooth muscle layer (SM); light blue: ventral mesenchymal pad in males (VMP) and paraurethral mesenchyme in females (PaM). D – V corresponds to the dorsoventral axis of the urethra. (i) Number, area, and perimeter of EB in one-day-old male and female gerbils (mean ± SEM; $n = 5$ prostate glands/group). *Statistically significant differences between control and Al group ($p \leq .05$). (For interpretation of the references to colour in this figure legend, the reader is referred to the web version of this article.)

i

	MALE		FEMALE	
	CONTROL	AI	CONTROL	AI
Buds number	9.0 ± 1.1	11.0 ± 1.0	3.4 ± 0.3	5.6 ± 0.4*
Area (µm^2)	14404.4 ± 1178	20416.0 ± 1007*	3800.9 ± 581.2	6066.2 ± 566.4*
Perimeter (µm)	1570.0 ± 67	2521.7 ± 380.1*	453.0 ± 60.5	793.4 ± 108.1*

Al group had an increasing of the body weight (Table 1).

3.2. Three-dimensional reconstruction of one-day-old animals

The ventral prostates (VP) of the control PN1 animals showed a normal developmental pattern (Fig. 2). In males, the epithelial buds (EB) elongated from the urethral epithelium following a V-shapped pattern, reaching the ventral mesenchymal pad (VMP) (Fig. 2a–b). In the female, a lower number of paraurethral EBs emerged from caudal urethra, heading linearly to the paraurethral mesenchyme (PaM), localized in a cranial position of the urethral segment, near the bladder neck (Fig. 2e–f). We found that the EBs may invade PaM unilaterally or bilaterally, although few EB reach the PaM (Fig. 2f).

Newborn males exposed to Al did not show an increase of the EB per sectional area (Fig. 2c–d; i). However, 3-D images showed an increase of smooth muscle (SM) gap surrounding the urethral (Fig. 2c–d). As expected, we observed that the ductal morphogenesis had a higher extension of the urethra in this experimental group (Fig. 2d). Moreover, the EB showed an area and a sectional perimeter significantly higher than that observed in control males (Fig. 2i).

Three dimensional analyses demonstrated that PN1 females exposed to Al had an apparent increase of PaM (Fig. 2g–h). These animals showed an increase in the number of the bilateral EB, area and sectional perimeter (Fig. 2i).

3.3. Morphology and stereology

PN1 males exposed to Al showed a higher relative frequency of EB and SM, and a decrease of mesenchymal compartment (Fig. 3a–b, Table 1). PN90 males of the Al group presented prostates with higher epithelial compartment (Fig. 4a), being surrounded by a thick smooth muscle layer (Fig. 4b). Stereology data demonstrated that VP of Al adult males had an increase in the epithelial and SM relative frequency (Table 1).

The urethra of Al newborn females showed a higher number of paraurethral EB, and a more vascularized mesenchyme (Fig. 5a–b).

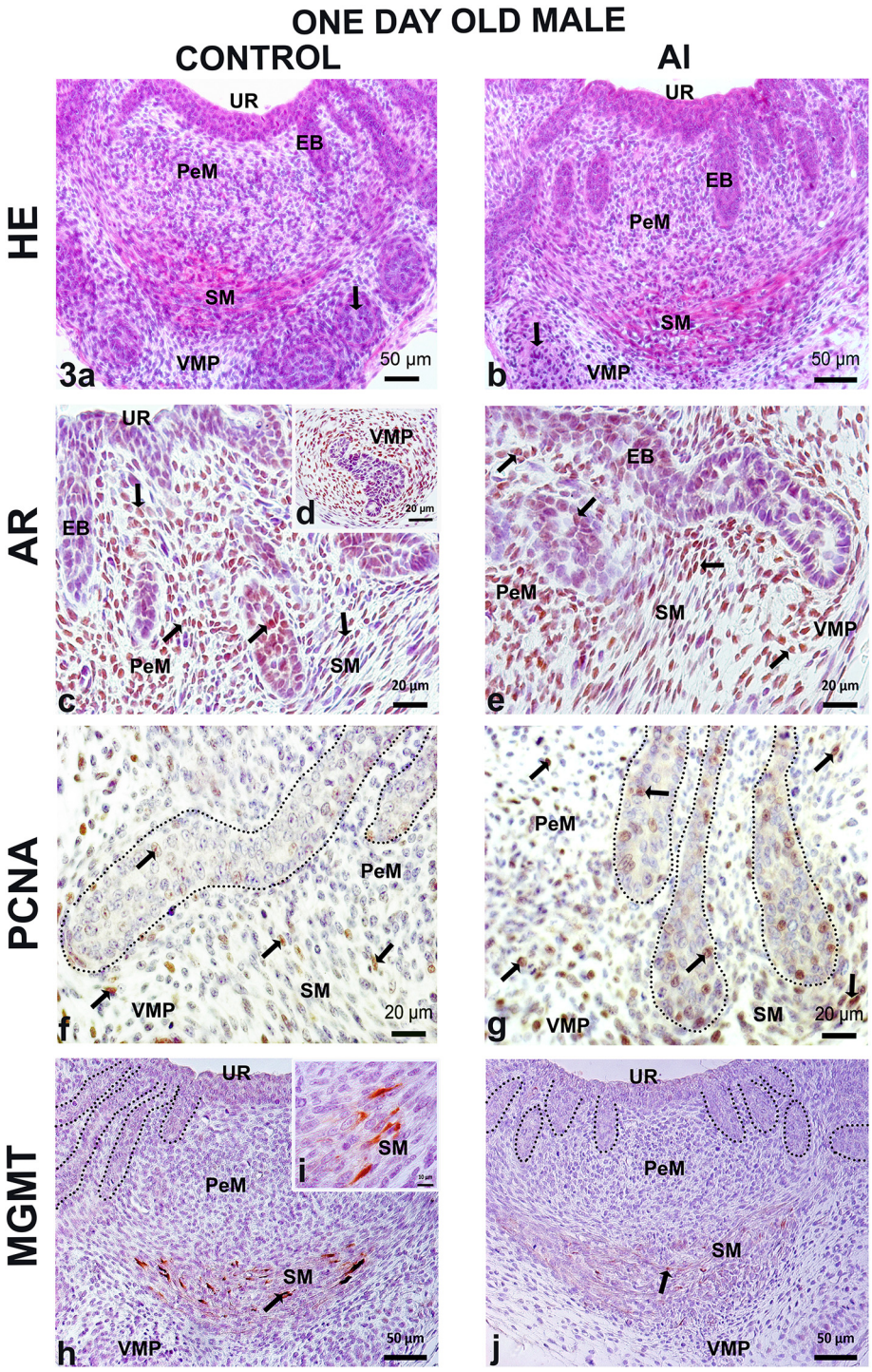

Fig. 3. Histological sections of ventral prostate in one-day-old male gerbils. (a, b) HE method showing the morphological aspects of this gland. Developing UGS is composed of the urethral epithelium (UR), which is surrounded by a layer of mesenchymal periurethral tissue (PeM) and a discontinuous layer of smooth muscle (SM). The ventral lobe of the gerbil prostate is composed of several solid epithelial cords (EB) that arise from the ventral UR epithelium, cross a gap in the SM, reaching the ventral mesenchymal pad (VMP). (c–e) AR-positive cells in EB, PeM, SM e VMP (arrows). (f–g) PCNA-positive cells in EB (dotted structures), PeM, SM e VMP (arrows). (h–j) Cytoplasmic staining for MGMT was observed in SM cells of the control and Al groups (arrows).

Stereological analysis showed that Al group had a significant increase of the relative frequency in epithelial compartment, and a decrease of the total mesenchyme (Table 1). We also observed that the prostate of Al adult females presented a higher epithelial development (Table 1), showing hyperplasic alveoli with several infolded-epithelial areas (Fig. 6a–b).

3.4. Immunohistochemical analyses

3.4.1. AR immunostaining

In both PN1 male group (control and Al) we observed AR-positive cells in EB, periurethral mesenchymae (PeM), SM, and VMP (Fig. 3c–e). We also noted a decreasing regarding the AR-positive cells in all VP compartments of treated newborn males. However, this reduction was significant only in PeM and VMP (Table 2). In PN90 males we did not observe differences regarding the immunostaining for AR between control and Al groups (Fig. 4c–d; Table 2).

All PN1 female prostate compartments (control and Al) showed AR-positive cells (Fig. 5d–e). For the Al group, the immunostaining decreased in all compartments, although only the EB had a significant reduction (Table 3). PN90 females exposed to Al showed a significant reduction of AR-positive cells in both epithelium and stroma (Fig. 6c–d; Table 3).

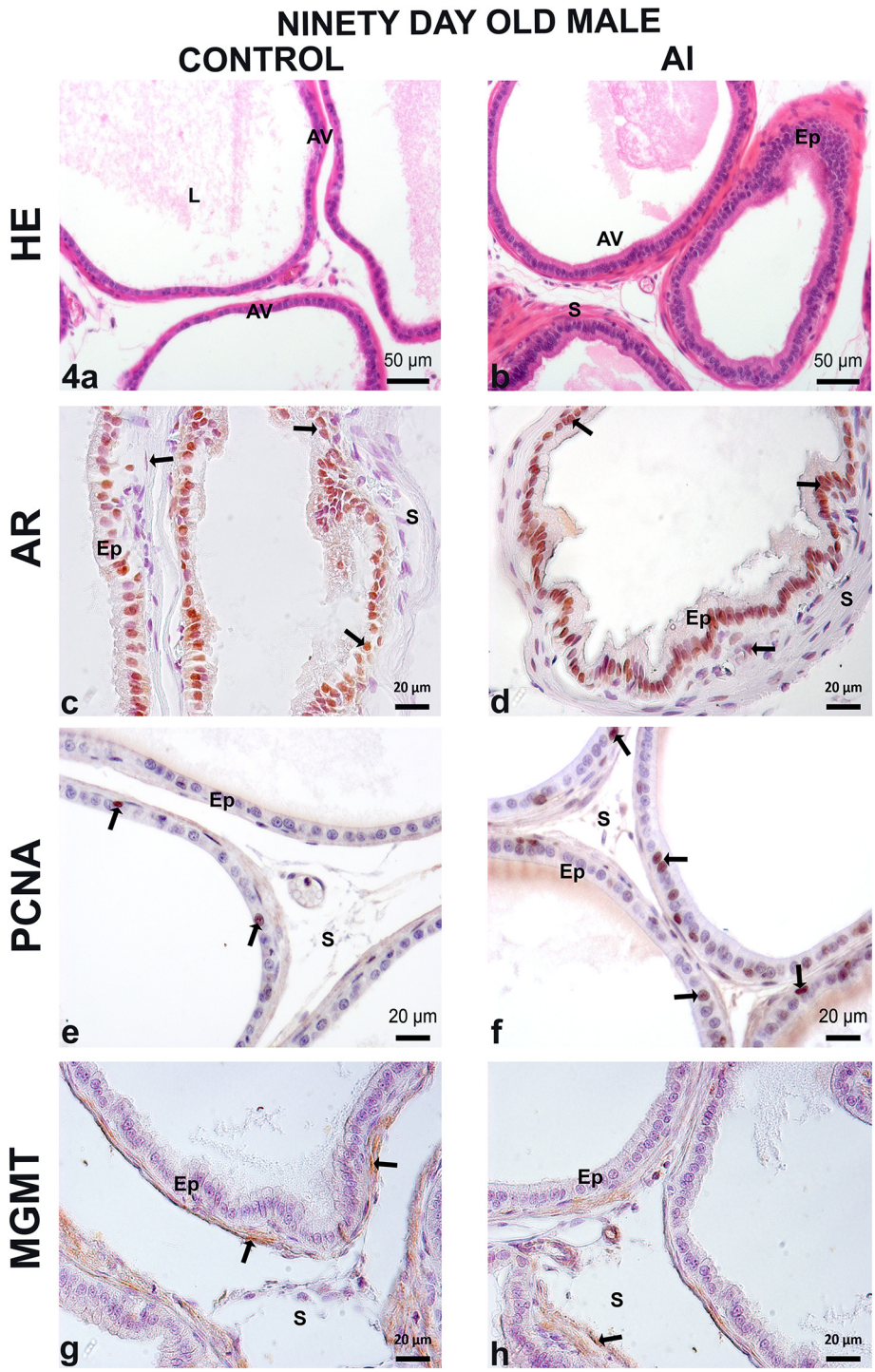

Fig. 4. Histological sections of the ventral prostate in adult male gerbils. (a–b) HE method showing morphological aspects of the ventral prostate in control and Al groups. In Al-treated gerbils the prostatic alveoli (AV) exhibited a more developed epithelium (Ep) and smooth muscle layer. Lumen (L), stroma (S). (c–d) AR-positive cells in Ep and S (arrows). (e–f) PCNA-positive cells in Ep and S (arrows). (g–h) Cytoplasmic staining for MGMT in smooth muscle layer (arrows).

3.4.2. ERα immunostaining

Regarding ERα immunostaining, we only detected ERα-positive cells in female prostates of PN1 and PN90 groups (Fig. 5f–g; Fig. 6e–f). These cells were observed in PeM, SM, and PaM of control and Al female groups (Fig. 5f–g). Quantitative analysis showed that the exposure to Al promoted a significant increase in the ERα staining in PeM, SM, and PaM (Table 3). Conversely, adult females demonstrated a significant reduction of this nuclear receptor in the stromal compartment (Fig. 6e–f; Table 3).

3.4.3. PCNA immunostaining

We detected PCNA-positive cells in EB, PeM, SM, and PaM compartments of PN1 male gerbils (Fig. 3f–g). However, for the Al-treated group these positive cells were more frequent (Table 2). PCNA-positive cells were also observed in epithelial and stromal compartments in VP in both control and Al PN90 males (Fig. 4e–f). However, the exposure to Al resulted in a significant increase of PCNA-positive cells only in prostatic epithelium (Table 2).

PN1 females presented prostates with PCNA-positive cells located in

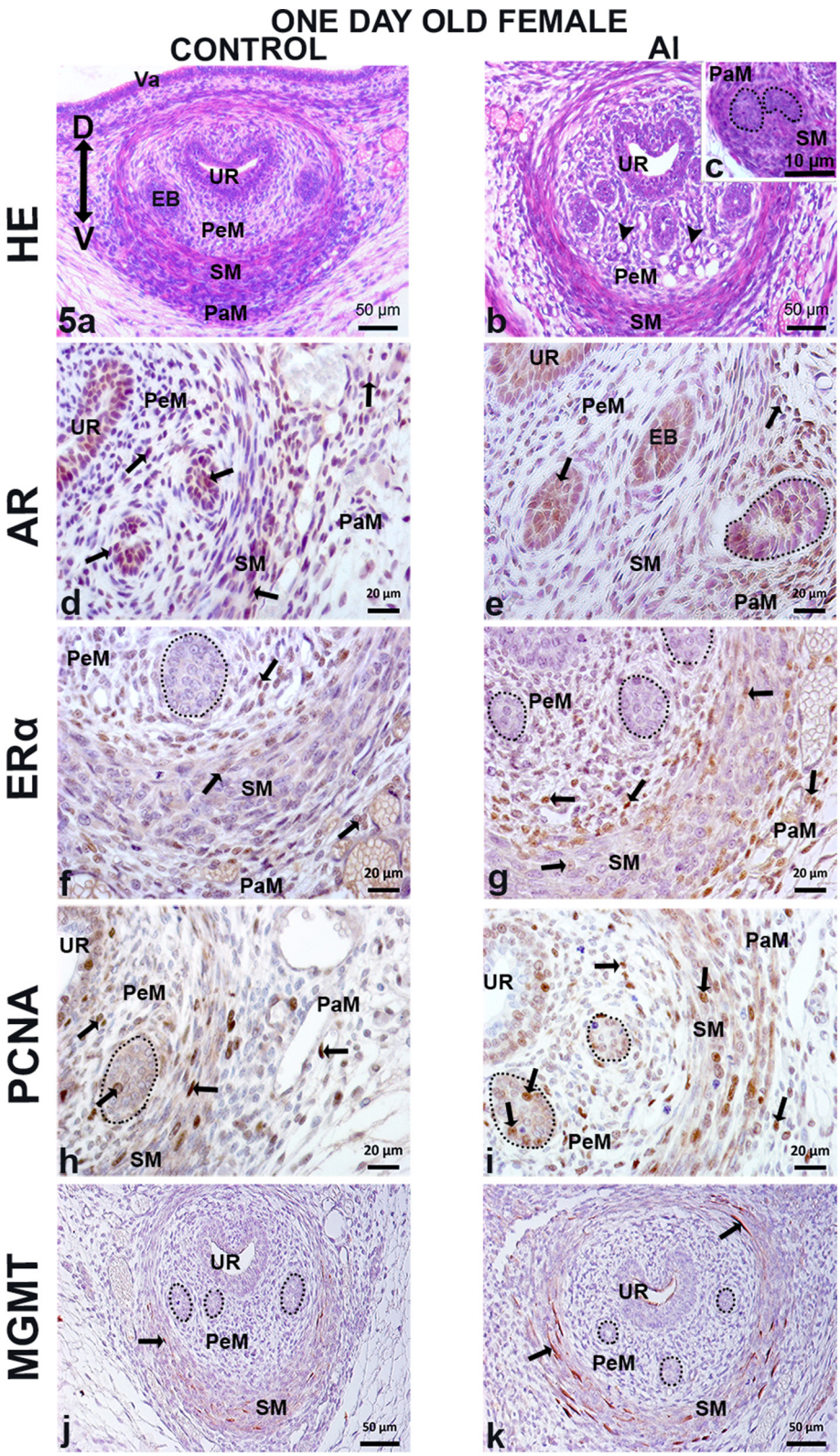

Fig. 5. Histological sections of paraurethral glands in one-day-old female gerbils. (a–c) HE method showing the morphological aspects of this gland. Developing UGS in female gerbils has similar structures to those observed in males of the same age. However, it can be seen that prostatic buds (EB, dotted structures) arise from the lateral sides of the caudal urethra (UR) and elongate within the periurethral mesenchyme (PeM) until reaching the paraurethral mesenchyme (PaM). Smooth muscle layer (SM); Blood vessels (arrowread). (d–e) AR-positive cells in BE, PeM, SM and PaM (arrows). (f–g) ERα-positive cells in PeM, SM and PaM (arrows). EB was negative for ERα (dotted lines). (h–i) PCNA-positive cells in PeM, BE (dotted), SM and PaM (arrows). (j–k) Cytoplasmic staining for MGMT was observed in SM cells of the control and Al groups (arrows).

EB, PeM, SM, and PaM (Fig. 5h–i). After exposure to Al, all these compartments became significantly more proliferative (Table 3). A significant increase of this immunostaining was also observed in epithelium and prostatic stroma of adult treated females (Fig. 6g–h; Table 3).

3.4.4. *MGMT immunostaining*

An intense cytoplasmic immunostaining for MGMT was observed in the smooth muscle cells of PN1 males (Fig. 3h–j). However, in PN1 males exposed to Al, this marking was weak and scattered (Fig. 3j). In both adult male groups, we observed a weak pattern of MGMT marking inside the smooth muscle cells surrounding prostatic alveoli (Fig. 4g–h).

In both PN1 females (control and Al) we also noted cytoplasmic

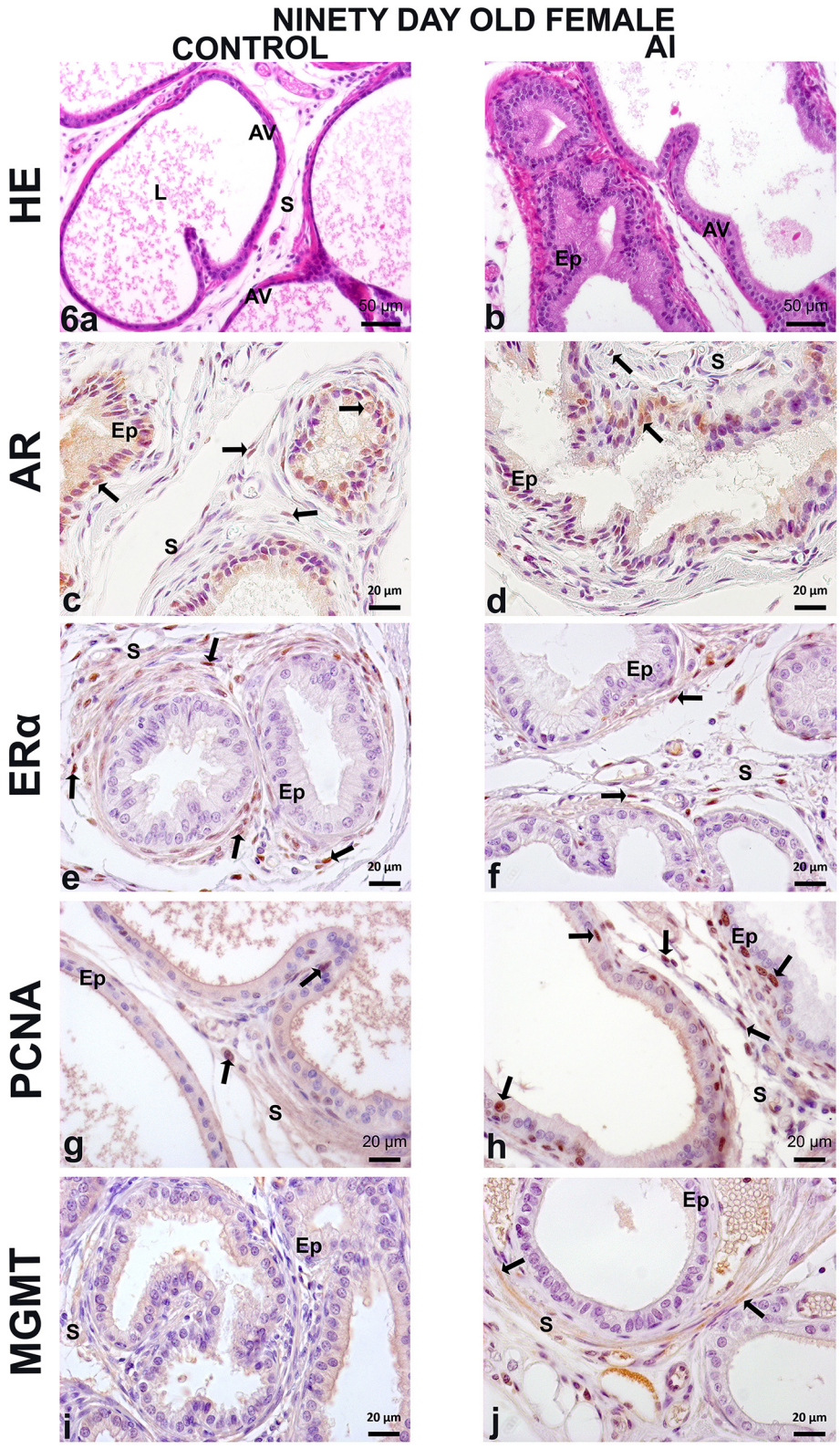

Fig. 6. Histological sections of the female prostate during adulthood. (a–b). HE method showing the morphological aspects of the female prostate. Al-treated glands exhibited proliferative alveoli (AV). Epithelium (Ep), stroma (S). (c–d) AR-positive cells in Ep and S (arrows). (e–f) ERα-positive cells in S (arrows). (g–h) PCNA-positive cells in Ep and S (arrows). (i–j) Weak cytoplasmic reaction for MGMT in smooth muscle cells of Al-treated female prostate.

reactions for MGMT in periurethral SM. However, these markings were more intense for the Al group (Fig. 5j–k). In adult female prostates, we noted weak cytoplasm reaction for MGMT in the periurethral SM (Fig. 6i–j).

3.5. Testosterone levels

Al-treatment caused a significant increase ($p \leq .05$) in serum testosterone levels of the PN90 male and female gerbils (Fig. 7).

Table 2
Frequency (%) of AR and PCNA-positive cells in the male gerbil prostate of all experimental groups.

	AR		PCNA	
	Control	Al	Control	Al
One-day-old				
EB	57.4 ± 4.0	47.0 ± 3.9	5.8 ± 0.7	28.1 ± 2.1*
PeM	79.4 ± 2.3	57.9 ± 2.2*	6.1 ± 0.8	10.6 ± 1.2*
SM	44.2 ± 4.1	33.9 ± 4.5	8.7 ± 0.8	23.2 ± 2.1*
VMP	86.0 ± 1.5	70.6 ± 3.1*	12.5 ± 1.2	15.4 ± 2.7
Ninety-days-old				
Epithelium	69.2 ± 4.4	61.2 ± 4.2	4.3 ± 0.5	14.7 ± 1.1*
Stroma	19.0 ± 1.5	18.5 ± 1.5	5.3 ± 0.8	8.2 ± 1.1

Epithelial buds (EB), periurethral mesenchyme (PeM), smooth muscle layer (SM), ventral mesenchymal pad (VMP). Values are means ± standard error of the means. Asterisks represent statistically significant differences between the experimental groups ($p \leq 0.05$; $n = 30$ fields in 3 animals/group).

4. Discussion

The results showed that Al prenatal exposure changes developmental patterns of the male and female gerbil prostates, promoting permanent modifications whose remain in adult life.

The Al dose employed in this study did not cause abortions or signs of external malformations. However, male and female gerbils exposed to Al showed a significant reduction of body weight at birth. This finding is an important indicative of the Al hazardous effects on the health, which has also been reported in studies that evaluated Al toxicity in rodent models (Hirata-Koizumi et al., 2011; Wang et al., 2012; Novaes et al., 2018).

Further, we also found a significant reduction of the female AGD, but not in males. The AGD is an efficient anthropometric measure to evaluate the toxic effects of endocrine-disrupting chemicals on the reproductive system (Liu et al., 2014). Some studies have been shown that decreased AGD is related with antiandrogenic drugs exposure (Castaño-Vinyals et al., 2012; Thankamony et al., 2016). This differential effect in males and females suggests that Al presents distinctive mechanisms of endocrine disruption in both genders, and also shows that the females seem to be more sensitive to this metal.

In general, three dimensional reconstruction and morphological data showed that Al exposure changed the prenatal prostate development in gerbils. PN1 prostates of females and males had an increase of the area, EB relative frequency, and PCNA-positive cells. Moreover, immunohistochemical data demonstrated a decreasing of AR immunostaining in both sexes, and an increase of the ERα-positive cells in females. Thus, the increase either of the epithelial proliferative index or in the EB area in Al-treated PN1 gerbils seems to be related with the modulation of androgenic and estrogenic receptors.

Previous studies have already reported several Al adverse effects on the reproductive system of rodents (Domingo, 1995; Marwa et al., 2017). In adult rats, Al exposure caused changes in the ovarian structure, and also decreased the expression of luteinizing hormone receptors (LHR) and follicle stimulating hormones receptors (FSHR), besides increasing the serological levels of testosterone and decreasing estradiol, progesterone, LH, and FSH (Wang et al., 2012; Fu et al., 2014). In rats and mice, testis toxicity was related with a decreasing in fertility and a lower AR expression (Guo et al., 2005; Sun et al., 2011; Makutina et al., 2014; Miska-Schramm et al., 2017). Although these studies have employed diverse methodologies, especially regarding the age, route and exposure dose, all them indicated that Al acts as an endocrine-disrupting chemical, changing either the serological hormonal levels or the expression of hormone receptors in gonads.

Although we have not succeed with ERα immunostaining in males, the decreased frequency for AR in both males and females, besides an increase of ERα in females, are indicatives that the Al also acted as an endocrine disruptor in PN1 gerbil prostate. The higher immunostaining for ERα in the prostatic mesenchymal cells can be associated with a higher cell proliferation, since an elevated ERα expression is correlated with higher cell proliferative index (Prins et al., 2001; Omoto et al., 2005).

Therefore, we suggest that Al acted as an antiandrogenic compound, blocking androgenic effects at AR level and modulating estrogenic receptor alpha in PN1 gerbil prostate. These findings corroborate with other *in vivo* and *in vitro* studies that demonstrated Al as a metalloestrogen, with potential to bind to estrogen receptors and to promote estrogen agonist responses (Martin et al., 2003; Darbre, 2006, 2009).

Prostate morphological changes found in PN1 animals seem to be permanent, since adult gerbils exposed to Al during intrauterine life showed higher levels of cell proliferation in both epithelial and stromal compartments. In addition, adult males and females showed high serum testosterone levels. However, the mechanisms that caused this glandular hyperplasia during adult life are unknown, since females and males showed different patterns of immunostaining for hormonal receptors.

In adult female prostate we observed a reduction of AR and ERα immunostaining. For adult males, we did not observe any changing regarding AR frequency. Thus, it is possible that Al has acted as a systemic endocrine disruptor, leading to changes in the regulation of the hyphotalamic-pituitary-gonadal axis. This hypothesis is supported by evidences found in other models that related Al as capable of changing the synthesis and releasing of pituitary hormones, thus disrupting steroidogenesis and gametogenesis (Domingo, 1995; Yousef et al., 2005; Wang et al., 2012; Zhu et al., 2014; Falana et al., 2017).

It is important to relate that we did not observe neoplastic lesions in adult prostates. However, Al-exposed females showed a higher immunostaining for O(6)-methylguanina-DNA meththyltransferase (MGMT) in the cytoplasm of smooth muscle cells. MGMT is an enzyme that works in DNA repairing, transferring methyl groups from DNA to an own cystein residue (Christmann et al., 2011; Gonçalves et al., 2013). Therefore, the higher immunostaining for MGMT in female

Table 3
Frequency (%) of AR, ERα, and PCNA-positive cells in the gerbil female prostate of all experimental groups.

	AR		ERα		PCNA	
	Control	Al	Control	Al	Control	Al
One-day-old						
EB	46.2 ± 4.1	26.2 ± 3.2*	–	–	3.8 ± 0.6	14.1 ± 0.9*
PeM	32.7 ± 2.7	28.2 ± 2.6	20.0 ± 3.1	48.7 ± 2.8*	10.9 ± 1.0	28.1 ± 1.2*
SM	22.6 ± 2.1	16.9 ± 3.0	12.3 ± 2.1	35.7 ± 2.1*	13.9 ± 2.0	29.1 ± 1.2*
PaM	67.4 ± 3.4	63.9 ± 3.8	48.4 ± 2.6	62.2 ± 1.7*	11.8 ± 1.5	29.9 ± 1.5*
Ninety-days-old						
Epithelium	41.2 ± 3.0	29.4 ± 3.3*	–	–	6.7 ± 1.0	15.6 ± 0.9*
Stroma	26.5 ± 2.4	17.8 ± 2.0*	66.0 ± 2.7	25.6 ± 3.7*	4.5 ± 0.5	16.6 ± 1.3*

Epithelial buds (EB), periurethral mesenchyme (PeM), smooth muscle layer (SM), paraurethral mesenchyme (PaM). Values are means ± standard error of the means. Asterisks represent statistically significant differences between the experimental groups ($p \leq 0.05$; $n = 30$ fields in 3 animals/group).

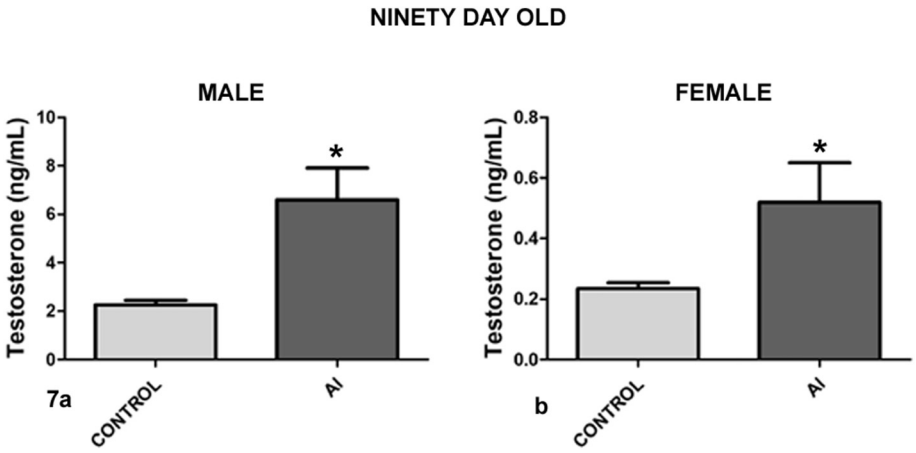

Fig. 7. Testosterone plasma levels (ng/mL) in control and Al-treated male and female adult gerbils (n = 6 animals/group). Values are mean ± standard error of mean. Asterisks represent statistically significant differences between the groups ($p \leq .05$).

prostates suggests that Al exposure results in a more susceptible status for epigenetic modifications. This way, new studies must be performed in order to evaluate the Al potential for causing epigenetic changes that can predispose this gland to lesions during aging.

Several studies performed by our group have demonstrated that the gerbil prostate is sensible to the action of endocrine-disrupting chemicals in different phases of prostate development (Perez et al., 2012; Biancardi et al., 2015; Campos et al., 2015; Lima et al., 2015; Perez et al., 2016). However, this is the first study that demonstrates the activity of Al as an endocrine-disrupting chemical on the male and female gerbil prostate. Therefore, the results of our study are important for public health, since Al exposure has been increased during last years, especially in newborn, child, and pregnant women (Crisponi et al., 2013; Fanni et al., 2014). Thus, these findings may be useful for public health policy organs in order to control Al employment in the pharmaceutical and food industry, as well as to warn about the risks of exposure to Al.

5. Conclusion

Al intrauterine exposure caused permanent alterations in development and morphophysiology of the male and female gerbil prostate. Body and prostatic changes were more pronounced in females than in males, suggesting sex-specific effects of the Al in gerbils. Our data indicate that Al promoted endocrine-disrupting responses in gerbils, modifying the modulation of the androgen and estrogen receptors in the prostate.

Conflict of interest

The authors declare that there are no conflicts of interest.

Acknowledgements

This paper was supported by a grant from Fundação de Amparo à Pesquisa do Estado de Goiás - Brazil (FAPEG, Nr. 08/2018). This study was financed in part by the Coordenação de Aperfeiçoamento de Pessoal de Nível Superior - Brasil (CAPES - Finance code 001).

References

Benett, R.W., Persaud, T.V.N., Moore, K.L., 1975. Experimental studies on the effects of aluminum on pregnancy and fetal development. Anat. Anz. Bd. 138, 365–378.
Biancardi, M.F., Perez, A.P., Caires, C.R., Góes, R.M., Vilamaior, P.S., Santos, F.C., Taboga, S.R., 2015. Prenatal exposure to testosterone masculinises the female gerbil and promotes the development of lesions in the prostate (Skene's gland). Reprod. Fertil. Dev. 27 (7), 1000–1011.
Callan, A.C., Hinwood, A.L., Ramalingam, M., Boyce, M., Heyworth, J., McCafferty, P., Odland, J.Ø., 2013. Maternal exposure to metals–concentrations and predictors of exposure. Environ. Res. 126, 111–117.
Campos, M.S., Galvão, A.L., Rodríguez, D.A., Biancardi, M.F., Marques, M.R., Vilamaior, P.S., Santos, F.C., Taboga, S.R., 2015. Prepubertal exposure to bisphenol-a induces ERα upregulation and hyperplasia in adult gerbil female prostate. Int. J. Exp. Pathol. 96 (3), 188–195.
Cardiano, P., Cigala, R.M., Crea, F., Giacobello, F., Giuffrè, O., Irto, A., Lando, G., Sammartano, S., 2017. Sequestration of Aluminium(III) by different natural and synthetic organic and inorganic ligands in aqueous solution. Chemosphere 186, 535–545.
Castaño-Vinyals, G., Carrasco, E., Lorent, J.A., Sabaté, Y., Cirac-Claveras, J., Pollán, M., Kogevinas, M., 2012. Anogenital distance and the risk of prostate cancer. BJU Int. 110, E707–E710.
Christmann, M., Verbeek, B., Roos, W.P., Kaina, B., 2011. O(6)-Methylguanine-DNA methyltransferase (MGMT) in normal tissues and tumors: enzyme activity, promoter methylation and immunohistochemistry. Biochim. Biophys. Acta 1816 (2), 179–190.
Crisponi, G., Fanni, D., Gerosa, C., Nemolato, S., Nurchi, V.M., Crespo-Alonso, M., Lachowicz, J.I., Faa, G., 2013. The meaning of aluminium exposure on human health and aluminium-related diseases. Biomol. Concepts. 4 (1), 77–87.
Darbre, P.D., 2006. Metalloestrogens: an emerging class of inorganic xenoestrogens with potential to add to the oestrogenic burden of the human breast. J. Appl. Toxicol. 26 (3), 191–197.
Darbre, P.D., 2009. Underarm antiperspirants/deodorants and breast cancer. Breast Cancer Res. 11, 3–S5.
Dhivya Bharathi, M., Justin-Thenmozhi, A., Manivasagam, T., Ahmad Rather, M., Saravana Babu, C., Mohamed Essa, M., Guillemin, G.J., 2018. Amelioration of aluminum maltolate-induced inflammation and endoplasmic reticulum stress-mediated apoptosis by tannoid principles of emblica officinalis in neuronal cellular model. Neurotox. Res. doi. https://doi.org/10.1007/s12640-018-9956-5. (Epub ahead of print).
Domingo, J.L., 1995. Reproductive and developmental toxicity of aluminum: a review. Neurotoxicol. Teratol. 17 (4), 515–521.
Erazi, H., Sansar, W., Ahboucha, S., Gamrani, H., 2016. Aluminum affects glial system and behavior of rats. C. R. Biol. 333 (1), 23–27.
Falana, B., Adeleke, O., Orenolu, M., Osinubi, A., Oyewopo, A., 2017. Effect of D-ribose-L-cysteine on aluminum induced testicular damage in male Sprague-Dawley rats. JBRA Assist. Reprod. 21 (2), 94–100.
Fanni, D., Ambu, R., Gerosa, C., Nemolato, S., Iacovidou, N., Van Eyken, P., Fanos, V., Zaffanello, M., Faa, G., 2014. Aluminum exposure and toxicity in neonates: a practical guide to halt aluminum overload in the prenatal and perinatal periods. World J. Pediatr. 10 (2), 101–107.
Fiala, J.C., 2005. Reconstruct: a free editor for serial section microscopy. J. Microsc. 218 (Pt 1), 52–61.
Flamini, M.A., Barbeito, C.G., Gimeno, E.J., Portiansky, E.L., 2002. Morphological characterization of the female prostate (Skene's gland or paraurethral gland) of Lagostomus maximus maximus. Ann. Anat. 184, 341–345.
Fu, Y., Jia, F.B., Wang, J., Song, M., Liu, S.M., Li, Y.F., Liu, S.Z., Bu, Q.W., 2014. Effects of sub-chronic aluminum chloride exposure on rat ovaries. Life Sci. 100, 61–66.
Gonçalves, B.F.G., Campos, S.G.P., Zanetoni, C., Scarano, W.R., Falleiros Jr., L.R., Amorim, R.L., Goes, R.M., Taboga, S.R., 2013. A new proposed rodent model of chemically induced prostate carcinogenesis: distinct time-course prostate cancer progression in the dorsolateral and ventral lobes. Prostate 73, 1202–1213.
Guo, C.H., Lu, Y.F., Hsu, G.S., 2005. The influence of aluminum exposure on male reproduction and offspring in mice. Environ. Toxicol. Pharmacol. 20, 135–141.
Hirata-Koizumi, M., Fujii, S., Ono, A., Hirose, A., Imai, T., Ogawa, K., Ema, M., Nishikawa, A., 2011. Two-generation reproductive toxicity study of aluminium sulfate in rats. Reprod. Toxicol. 31 (2), 219–230.
Hond, E.D., Schoeters, G., 2006. Endocrine disrupters and human puberty. Int. J. Androl. 29 (1), 264–271.

Lifeng, Z., Cuihong, J., Qiufang, L., Xiaobo, L., Shengwen, W., Jinghua, Y., Yanqiu, D., Linlin, Z., Yuan, C., 2013. Effects of subchonic aluminum exposure on spatial memory, ultrastructure and L-LTP of hippocampus in rats. J. Toxicol. Sci. 38 (2), 255–268.

Lima, R.F., Rodriguez, D.A., Campos, M.S., Biancardi, M.F., Santos, I.F., Oliveira, W.D., Cavasin, G.M., Marques, M.R., Taboga, S.R., Santos, F.C., 2015. Bisphenol-A promotes antiproliferative effects during neonatal prostate development in male and female gerbils. Reprod. Toxicol. 58, 238–245.

Liu, C., Xu, X., Huo, X., 2014. Anogenital distance and its application in environmental health research. Environ. Sci. Pollut. Res. Int. 21 (8), 5457–5464.

Makutina, V.A., Balezin, S.L., Slyshkina, T.V., Pashnina, I.A., Likhacheva, E.I., 2014. Experimental evaluation of combined effects caused by stress and metals (cadmium and aluminium) in reproductivity of male rats. Med. Tr. Prom. Ekol. 6, 30–34.

Marker, P.C., Donjacour, A.A., Dahiya, R., Cunha, G.R., 2003. Hormonal, cellular, and molecular control of prostatic development. Dev. Biol. 253, 165–174.

Martin, M.B., Reiter, R., Pham, T., Avellanet, Y.R., Camara, J., Lahm, M., Pentecost, E., Pratap, K., Gilmore, B.A., Divekar, S., Dagata, R.S., Bull, J.L., Stoica, A., 2003. Estrogen-like activity of metals in Mcf-7 breast cancer cells. Endocrinology 144, 2425–2436.

Marwa, M., Adrian, F., Nedra, B., Samira, M., Horea, M., Walid-Habib, T., Baati, R., Leila, T., 2017. The role of lysosomes in the phenomenon of concentration of aluminum and indium in the female reproductive system. An ultrastructural study. J. Trace Elem. Med. Biol. 44, 59–64.

Miska-Schramm, A., Kapusta, J., Kruczek, M., 2017. The effect of aluminum exposure on reproductive ability in the bank vole (*Myodes glareolus*). Biol. Trace Elem. Res. 177 (1), 97–106.

Mouro, V.G.S., Menezes, T.P., Lima, G.D.A., Domingues, R.R., Souza, A.C.F., Oliveira, J.A., Matta, S.L.P., Machado-Neves, M., 2018. How bad is aluminum exposure to reproductive parameters in rats? Biol. Trace Elem. Res. 183 (2), 314–324.

Nampoothiri, M., Ramalingayya, G.V., Kutty, N.G., Krishnadas, N., Rao, C.M., 2017. Insulin combined with glucose improves spatial learning and memory in aluminum chloride-induced dementia in rats. J. Environ. Pathol. Toxicol. Oncol. 36 (2), 159–169.

Novaes, R.D., Mouro, V.G.S., Gonçalves, R.V., Mendonça, A.A.S., Santos, E.C., Fialho, M.C.Q., Machado-Neves, M., 2018. Aluminum: a potentially toxic metal with dose-dependent effects on cardiac bioaccumulation, mineral distribution, DNA oxidation and microstructural remodeling. Environ. Pollut. 242 (Pt A), 814–826.

Oda, S.S., 2016. The influence of Omega3 fatty acids supplementation against aluminum-induced toxicity in male albino rats. Environ. Sci. Pollut. Res. Int. 23 (14), 14354–14361.

Omoto, Y., Imamov, O., Warner, M., Gustafsson, J.A., 2005. Estrogen receptor alpha and imprinting of the neonatal mouse ventral prostate by estrogen. Proc. Natl. Acad. Sci. 102 (5), 1484–1489.

Perez, A.P., Biancardi, M.F., Vilamaior, P.S., Góes, R.M., Santos, F.C., Taboga, S.R., 2012. Microscopic comparative study of the exposure effects of testosterone cypionate and ethinylestradiol during prenatal life on the prostatic tissue of adult gerbils. Microsc. Res. Tech. 75 (8), 1084–1092.

Perez, A.P., Biancardi, M.F., Caires, C.R., Falleiros-Junior, L.R., Góes, R.M., Vilamaior, P.S., Santos, F.C., Taboga, S.R., 2016. Prenatal exposure to ethinylestradiol alters the morphologic patterns and increases the predisposition for prostatic lesions in male and female gerbils during ageing. Int. J. Exp. Pathol. 97 (1), 5–17.

Prins, G.S., Birch, L., Couse, J.F., Choi, I., Katzenellenbogen, B., Korach, K.S., 2001. Estrogen imprinting of the developing prostate gland is mediated through stromal estrogen receptor alpha: Studies with alpha ERKO and beta ERKO mice. Cancer Res. 61, 6089–6097.

Prins, G.S., Tang, W.Y., Belmonte, J., Ho, S.M., 2008. Perinatal exposure to oestradiol and bisphenol A alters the prostate epigenome and increases susceptibility to carcinogenesis. Basic Clin. Pharmacol. Toxicol. 102 (2), 134–138.

Sanches, B.D., Biancardi, M.F., Dos Santos, F.C., Goes, R.M., Vilamaior, P.S., Taboga, S.R., 2014. Budding process during the organogenesis of the ventral prostatic lobe in mongolian gerbil. Microsc. Res. Tech. 77, 458–466.

Santos, F.C., Leite, R.P., Custódio, A.M., Carvalho, K.P., Monteiro-Leal, L.H., Santos, A.B., Góes, R.M., Carvalho, H.F., Taboga, S.R., 2006. Testosterone stimulates growth and secretory activity of the female prostate in the adult gerbil (*Meriones unguiculatus*). Biol. Reprod. 75 (3), 370–379.

Sun, H., Hu, C., Jia, L., Zhu, Y., Zhao, H., Shao, B., Wang, N., Zhang, Z., Li, Y., 2011. Effects of aluminum exposure on serum sex hormones and androgen receptor expression in male rats. Biol. Trace Elem. Res. 144 (1–3), 1050–1058.

Thankamony, A., Pasterski, V., Ong, K.K., Acerini, C.L., Hughes, I.A., 2016. Anogenital distance as a marker of androgen exposure in humans. Andrology 4 (4), 616–625.

Vilamaior, P.S., Taboga, S.R., Carvalho, H.F., 2006. Postnatal growth of the ventral prostate in Wistar rats: a stereological and morphometrical study. Anat Rec A Discov Mol Cell Evol Biol 288 (8), 885–892.

Wang, N., She, Y., Zhu, Y., Zhao, H., Shao, B., Sun, H., Hu, C., Li, Y., 2012. Effects of subchronic aluminum exposure on the reproductive function in female rats. Biol. Trace Elem. Res. 145 (3), 382–387.

Weibel, E.R., 1963. Principles and methods for the morphometric study of the lung and other organs. Lab. Investig. 12, 131–155.

Yokel, R.A., McNamara, P.J., 2001. Aluminum toxicokinetics: an updated minireview. Pharmacol. Toxicol. 88 (4), 159–167.

Yousef, M.I., Morsy, A.M.A., Hassan, M.S., 2005. Aluminium-induced deterioration in reproductive performance seminal plasma biochemistry of male rabbits: protective role of ascorbic acid. Toxicology 215, 97–107.

Zahedi-Amiri, Z., Taravati, A., Hejazian, L.B., 2018. Protective effect of rosa damascena against aluminum chloride-induced oxidative stress. Biol. Trace Elem. Res. doi. https://doi.org/10.1007/s12011-018-1348-4. (Epub ahead of print).

Zaviacic, M., Ablin, R.J., 2000. The female prostate and prostate-specific antigen. Immunohistochemical localization, implications of this prostate marker in women and reasons for using the term "prostate" in the human female. Histol. Histopathol. 15 (1), 131–142.

Zhu, Y.Z., Sun, H., Fu, Y., Wang, J., Song, M., Li, M., Li, Y.F., Miao, L.G., 2014. Effects of sub-chronic aluminum chloride on spermatogenesis and testicular enzymatic activity in male rats. Life Sci. 102, 36–40.

Zhu, Y., Hu, C., Zheng, P., Miao, L., Yan, X., Li, H., Wang, Z., Gao, B., Li, Y., 2016. Ginsenoside Rb1 alleviates aluminum chloride-induced rat osteoblasts dysfunction. Toxicology 10 (368–369), 183–188.